Speed Sensorless Mixed Sensitivity Lpv H_∞ Control of the Induction Motor

R. Tóth , D. Fodor

University of Veszprém, Department of Automation
Egyetem Street 10., Veszprém, Hungary
URL: http://www.vein.hu, e.mail: fodor@almos.vein.hu

***Abstract* – The paper shows the design of a robust control structure for the speed sensorless vector control of the IM, based on the mixed sensitivity linear parameter variant (LPV) H_∞ theory. The controller makes possible the direct control of the flux and speed of the motor with torque adaptation in noisy environment. The whole control system is tested by intensive simulations and according to the results shows good dynamic and robust performance. Implementation issues based on a DSP TMS320F243 development platform are also presented.**

***Index Terms* – inductor motor, LPV, speed sensorless, gain scheduling control, H_∞, mixed sensitivity.**

I. INTRODUCTION

Induction motors (IM) are widely used in the industry due to their simple structure, low cost, and high reliability. Although they are the horsepower of industry, their control is significantly more challenging than of d. c. motors, because as a dynamical system they have a highly nonlinear nature with parameter disturbances. This is the reason, why IMs are still not rival to their d. c. cousins in a number of high precision applications. Nowadays, therefore, there is a great interest in developing high performance and robust controllers to make induction drives unbeatable in all fields of applications. Especially, these efforts concentrate on controllers that do not need speed sensors to operate, which greatly reduces costs and maintenance. (For details see [5, 13]).

Motivated by this goal, we show the design steps of a robust controller for speed sensorless operation of IMs. The designed system gives the opportunity of fast control of the speed of the motor and the magnetic field associated with the rotor flux ($\boldsymbol{\Psi}_r = \left[\Psi_{rd}, \Psi_{rq}\right]^T$). This system also possesses the ability to operate in noisy environment and the online adaptation to the load torque (T_{load}), which is significant for dynamic tasks. The implemented control law is based on the linear parameter variant (LPV) theory of H_∞ control with mixed sensitivity (MS), which has recently appeared in this field [8, 10]. The controller is supported by an I/O linearized reference model and a complex observer synthesized from an extended Kalman filter (EKF) [1, 6] and a H_∞ observer [3, 11]. This structure needs only the measurements of the stator currents, and it shows robustness against system and measurement noises. Moreover, the proposed control law is designed to be easy to tune, that holds the possibility of the online tuning of the performance.

The paper is organized as follows. The LPV model of the induction motor is given in *Section 2*, the theory of MS LPV H_∞ control in *Section 3*. The design steps of the controller are given in *Section 4* and *Section 5* includes the simulated results. The implementation with a digital signal processor (DSP) is presented in *Section 6* and finally the conclusions are given in *Section 7*.

II. LPV MODEL OF THE INDUCTION MOTOR

In case of assuming that every variable is continually distributed inside of the machine and magnetic properties of the rotor are ideal, and using phasor theory to describe the density distribution of the electrical quantities and magnetic fields around the stator and the rotor. (For details see [4, 7]), than the mathematical model of the squirrel-cage IM can be easily derived,. The relationship between the flux density, describing the magnetic field, the stator current ($\mathbf{i}_s = \left[i_{sd}, i_{sq}\right]^T$), and the stator voltage ($\mathbf{u}_s = \left[u_{sd}, u_{sq}\right]^T$) can be realized through 2 differential and 2 algebraic equation where the uncertainty of the rotor resistance (R_r) introduces nonlinearity into the system. From these equations the (2.1) system follows. This is called the stator oriented (α,β) model of the IM, without the motion equation.

$$\frac{d}{dt}\begin{bmatrix}\Psi^{s}_{r\alpha}\\ \Psi^{s}_{r\beta}\\ i^{s}_{s\alpha}\\ i^{s}_{s\beta}\end{bmatrix}=\begin{bmatrix}-\Psi^{s}_{r\alpha}/T_r-\omega\Psi^{s}_{r\beta}+L_m i^{s}_{s\alpha}/T_r\\ \omega\Psi^{s}_{r\alpha}-\Psi^{s}_{r\beta}/T_r+L_m i^{s}_{s\beta}(t)/T_r\\ \tau\Psi^{s}_{r\alpha}/(\sigma T_r)+\omega\cdot\tau\Psi^{s}_{r\beta}/\sigma-(\lambda T_r+T_s)i^{s}_{s\alpha}/\sigma\\ -\omega(t)\cdot\tau\Psi^{s}_{r\alpha}/\sigma+\tau\Psi^{s}_{r\beta}/(\sigma T_r)-(\lambda T_r+T_s)i^{s}_{s\beta}/\sigma\end{bmatrix}+\begin{bmatrix}0 & 0\\ 0 & 0\\ 1/\sigma L_s & 0\\ 0 & 1/\sigma L_s\end{bmatrix}\cdot\begin{bmatrix}u^{s}_{s\alpha}\\ u^{s}_{s\beta}\end{bmatrix},\quad(2.1)$$

$$\underbrace{\frac{d}{dt}\begin{bmatrix}\Psi^{fr}_{rd}\\ i^{fr}_{sd}\\ i^{fr}_{sq}\end{bmatrix}}_{\dot{x}}=\underbrace{\begin{bmatrix}-p_2/L_r & L_m p_2/L_r & 0\\ \lambda p_2/(L_r\sigma) & -(\lambda p_2/L_r+T_s)/\sigma & p_3\\ -\lambda p_1/\sigma & -p_3 & -(\lambda p_2/L_r+T_s)/\sigma\end{bmatrix}}_{A(p)}\cdot\begin{bmatrix}\Psi^{fr}_{rd}\\ i^{fr}_{sd}\\ i^{fr}_{sq}\end{bmatrix}+\underbrace{\begin{bmatrix}0 & 0\\ 1/\sigma L_s & 0\\ 0 & 1/\sigma L_s\end{bmatrix}}_{B}\cdot\underbrace{\begin{bmatrix}u^{fr}_{sd}\\ u^{fr}_{sq}\end{bmatrix}}_{u},\quad(2.2)$$

where the parameters are defined as follows: $\sigma=1-L_m^2/(L_sL_r)$, $\lambda=L_m^2/L_s$, $\tau=L_m/(L_sL_r)$, $T_r=L_r/R_r$, $T_s=L_s/R_s$ and their nominal values are given in *Table 1*.

If we approximate R_r with equation (2.3) based on the theory of heating materials (aluminium) with linear convection (K_k) of heat [12]:

$$\frac{dR_r}{dt}=\underbrace{\frac{0.86\cdot R_0}{(245+T_0)\cdot m\cdot c}}_{R_{T0}}\cdot\left(i^{r}_{eff}\right)^2\cdot R-K_k(R_r-R_0),\quad(2.3)$$

then with the rotor field orientation (RFO) of the phasors [7] the LPV model of the IM is the following:

which is an input affine representation where only the state matrix **A** is dependent on the

$$\mathbf{p}:\mathbb{R}_+\to\mathbb{R}^3_+=[p_1(t)\ \ p_2(t)\ \ p_3(t)]^T=[\omega(t)\ \ R_r(t)\ \ \omega_{rflux}(t)]^T,\quad(2.4)$$

parameters with the polytopic set given in *Table 1*. These parameters are defined as follows: The angular speed $\omega(t)$ of the IM is given by the dynamic motion equation (2.5) of the rotor.

$$\frac{d\omega}{dt}=\frac{3p^2L_m}{2JL_r}\cdot\left(\Psi^{fr}_{rd}\cdot i^{fr}_{sq}\right)-\frac{p}{J}\cdot(T_{load}+F\omega),\quad(2.5)$$

R_r is given by (2.3) and

$$\omega_{rflux}(t)=\omega(t)+\left(L_m R_r(t)\cdot i^{fr}_{sq}(t)\right)/\left(L_r\Psi^{fr}_{rd}(t)\right).\quad(2.6)$$

It is important to note that this RFO LPV model of the IM, gives the possibility to independently control the flux with i^{fr}_{sd} (see (2.2)) and ω with i^{fr}_{sq} (see (2.5)). This principle is the cornerstone of our algorithm.

III. Mixed Sensitivity LPV H_∞ Theory

3.1 H_∞ theory - From the germinal works of Zames [14] to the highly improved theories of the MS MIMO controls [27, 31], the H_∞ theory has conquered great portion of today's controller designs with lots of implemented examples [8, 9, 10]. Let us give a brief outline of this theory:

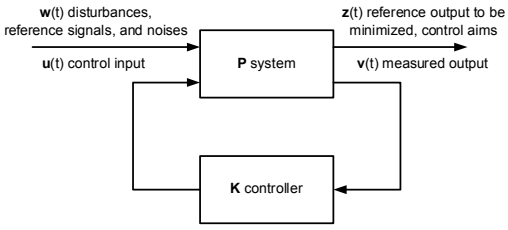

Fig. 1. General problem definition

Having a general control structure with system **P** as in *Figure 1*, we are searching an optimal, robust, and stabilizing controller **K** that minimalizes the H_∞ norm of the system:

$$\left\|\mathbf{G}(\mathbf{P},\mathbf{K})(s)\right\|_\infty=\sup_{\|\mathbf{w}(t)\|_2\neq 0}\frac{\|\mathbf{z}(t)\|_2}{\|\mathbf{w}(t)\|_2},\quad t\in(0,\infty).\quad(3.1)$$

This optimalization is usually solved by a γ-iteration instead of a direct minimalization. In each recursive step of this iteration we are looking for a controller fulfilling (3.2).

$$\left\|\mathbf{G}(\mathbf{P},\mathbf{K})\right\|_\infty<\gamma.\quad(3.2)$$

In practice, (3.2) is solved based on the Ricatti equations or linear matrix inequalities (LMIs). The next γ is computed from the pervious step until we get close enough to its optimal value. It is proved that this algorithm converges and produces a robust controller which is stable and fulfills (3.2) on the whole frequency spectrum [15].

3.2 LPV systems - The LPV systems are such linear systems, where the $\mathbf{A}(.)$ … $\mathbf{D}(.)$ matrices in the state-space representation are dependent on a $\mathbf{p}(t)\in\mathbb{R}^n$ parameter vector.

$$\dot{\mathbf{x}} = \mathbf{A}(\mathbf{p})\mathbf{x} + \mathbf{B}(\mathbf{p})\mathbf{u}$$
$$\mathbf{y} = \mathbf{C}(\mathbf{p})\mathbf{x} + \mathbf{D}(\mathbf{p})\mathbf{u} \qquad (3.4)$$

Further an LPV system can be imagined as a point by point LTI system moving in a n dimensional system space. Supposing that the **p** vector is bounded (Condition#1) and the system is affine in **p** (Condition#2), then each of the $\mathbf{A}(.)$ … $\mathbf{D}(.)$ matrices can be transformed into an $\mathbf{X}(\mathbf{p}) = \mathbf{X}_0 + \mathbf{X}_1(p_1) + \ldots \mathbf{X}_n(p_n)$ form. These systems can be described by an n dimensional cube which can be transformed into a polytope (*see Figure 3*) defined (existing) on a 2 dimensional system space.

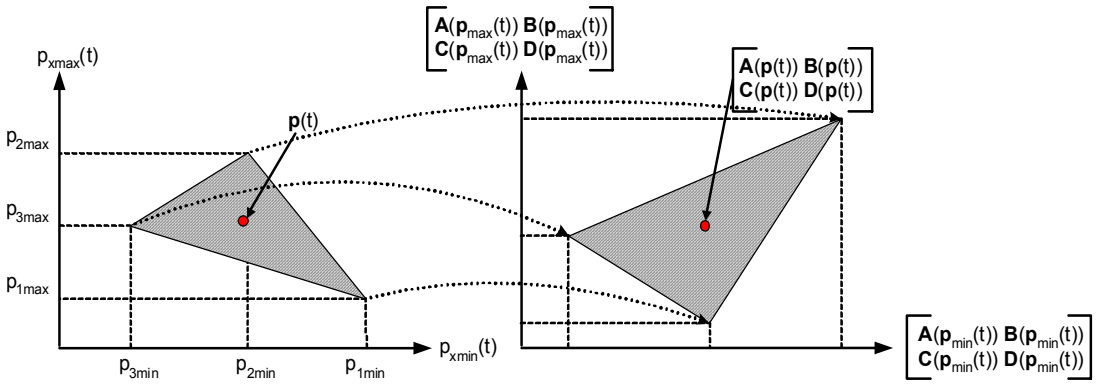

Fig. 2. Polytope form of p(t)

Fig. 3. Polytope form of a LPV system dependent on p(t)

If system **P** can be represented with such a polytope, and the closed loop system fulfills (3.2) for a given γ than an LPV H_∞ controller can be computed for each corner of the polytope set **P.** In practice this is done through LMIs. In this way, an LPV H_∞ controller can be designed for the LPV model of the IM, because (2.2) fulfils Condition#1 and Condition#2.

3.3 Mixed sensitivity - By introducing frequency filters (weighting functions) on the I/O signals of the system, not only the model of the IM can be more accurately defined, but the properties of the designed controller can be also directly influenced. The robust stability, disturbance and noise attenuation, and reference tracking of the whole system can be defined, with the frequency definition of the sensitivity function $\mathbf{S} = (\mathbf{I} + \mathbf{GK})^{-1}$, the inverse sensitivity function $\mathbf{T} = \mathbf{I} - \mathbf{S}$, and the closed loop transfer function **KS.** For a reference tracking objective, the structure presented on *Figure 4* shall be considered. Here, each of the previously mentioned transfer functions are influenced by the $\mathbf{W}_S$, $\mathbf{W}_T$, $\mathbf{W}_{KS}$ filters, where $\mathbf{W}_S$ must be a low-pass filter for good reference tracking, $\mathbf{W}_T$ must be a high-pass filter for good noise attenuation, and $\mathbf{W}_{KS}$ must be a high-pass filter for robust stability and disturbance attenuation. Moreover, the presented $\mathbf{W}_d$ and $\mathbf{W}_r$ should be low-pass filters to define the frequency domain of the input signals. If such a structure considered for a H_∞ control objective, then the γ-iteration will find a **K** controller that minimalizes (3.5).

$$\left\| \mathbf{G}(\mathbf{P},\mathbf{K}) \right\|_\infty = \left\| \begin{bmatrix} \mathbf{W}_S\mathbf{S} \\ \mathbf{W}_T\mathbf{T} \\ \mathbf{W}_{KS}\mathbf{KS} \end{bmatrix} \right\|_\infty \qquad (3.5)$$

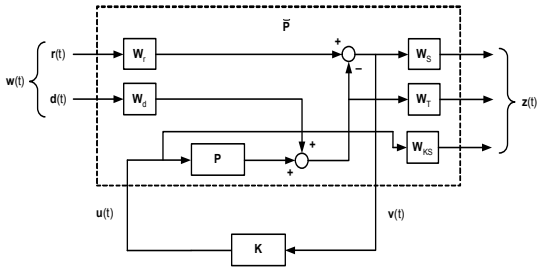

Fig. 4. Mixed sensitivity tracking structure

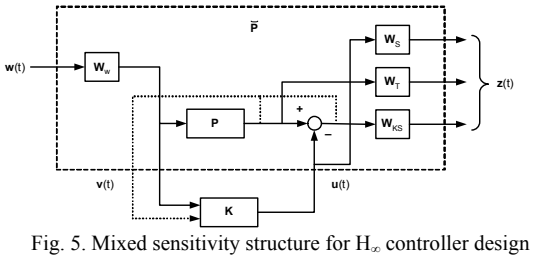

Fig. 5. Mixed sensitivity structure for H_∞ controller design for H_∞ observer design

For estimation objective by H_∞ observers, in a similar manner a MS structure is given on *Figure 5*.

IV. SPEED SENSORLESS CONTROLLER DESIGN

To fulfill the above requirements for an IM drive, the controller structure in *Figure 6* has been proposed. This structure provides the independent control of the speed and flux based only on the measurement of the stator currents. The measured noisy 3-phase stator currents are transformed to their vectorial representation with the Clark transformation [7], and than they are cleaned from the noise by a complex estimation structure, which is the interconnection of a H_∞ observer and a Kalman filter [1, 6]. The Kalman filter provides the estimation of ω and R_r from the nonlinear equations of the model: (2.3), (2.5), and the H_∞ observers provides the stator oriented estimation of the rotor flux (Ψ_r^s), which is needed for the RFO. After RFO, the input reference signals, Ψ_{ref}, ω_{ref} are transformed to current references, $i_{sd_{ref}}^{fr}$ and $i_{sq_{ref}}^{fr}$, by the help of an I/O linearized model of the IM and based on the previously calculated ω, R_r, Ψ_{rd}^{fr}, i_{sd}^{fr}, and i_{sq}^{fr}. The H_∞ controller gets the deviation $i_{sd(error)}^{fr}$, $i_{sq(error)}^{fr}$, from the current reference and calculates the new voltage phasor, which is transformed to 3-phase by the Space Vector Pulse Width Modulation (SVPWM) element that directly controls the firing impulses of the 3 phase inverter realizing the desired value of the stator voltage for IM.

The H_∞ controller was designed with the following MS structure for the LPV model of the IM ((2.2)).

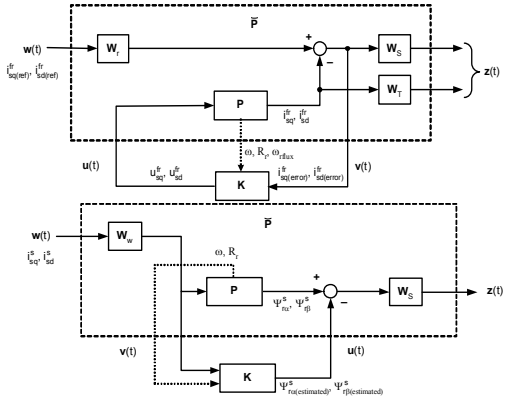

Fig. 7. MS structure for H_∞ tracking, Fig. 8. MS structure for the H_∞ flux observer

This structure inhabits a very rapid control ability of the flux and the speed through the stator current reference. During the design the sensitivity filter $\mathbf{W}_S$ was chosen to be

$$\mathbf{W}_S(s) = \mathrm{diag}\left(10/(s+10), 10/(s+10)\right), \quad (4.1)$$

providing good reference tracking on low frequency deviations and preventing the controller to be unnecessary aggressive beyond the cutting-off frequency. The amplification of the filter is only 1dB in the passing region, which gives the possibility to tune the speed and accuracy of the control by external amplification of the current reference signals. Because we greatly reduced the uncertainty by the estimation of R_r, there is no need to choose a dynamic filter for $\mathbf{W}_T$. By trial and error $\mathbf{W}_T$ was designed to be

$$\mathbf{W}_T(s) = \mathrm{diag}\left(0.8, 0.8\right). \quad (4.2)$$

For $\mathbf{W}_r$ the following filter was introduced to restrict the speed of reference tracking which prevents the controller to be unstable even to the step like changes of the reference signals.

$$\mathbf{W}_r(s) = \mathrm{diag}\left(15/s+15,\ 15/s+15\right), \quad (4.3)$$

Almost the half of $T_{r0} = L_r / R_0 = 43\mathrm{msec}$ for T_{W_r} has provided good tracking without significant overshoots. It is important to note, that because this structure was designed without an integrator than an off-set error is expected. In opposite to the common practice, this makes possible the external tuning of the controller without destabilizing the whole system.

The optimalization was computed through the Matlab function *hinfgs* which is the part of the LMI toolbox. The resulted controller had 5 states, with two inputs and outputs, and it was described with $2^3 = 8$ LTI corner systems, with $\gamma = 0.6247$. This means, that without external amplification of $i_{sd(error)}^{fr}$ and $i_{sq(error)}^{fr}$ the steady state off-set error is 62.47%.

The I/O linearization of (2.2) gives us the possibility to transform Ψ_{ref}, ω_{ref} into $i_{sd_{ref}}^{fr}$ and $i_{sq_{ref}}^{fr}$. If the derivatives of Ψ_{rd}^{fr} and ω are chosen to v_1, v_2 virtual inputs equal to Ψ_{ref}, ω_{ref} than the following algebraic equation system provides the reference computation:

$$i_{sd_{ref}}^{fr} = L_r v_1 / \left(L_m R_r\right) + \Psi_{rd}^{fr} / L_m, \tag{4.4}$$

$$i_{sq_{ref}}^{fr} = T_{mech} v_2 / \left(p \cdot \Psi_{rd}^{fr}\right) + T_{mech}\left(T_{load} + F\omega\right), \text{ where } T_{mech} = 2JL_r / 3pL_m. \tag{4.5}$$

The (4.4) and (4.5) equations can handle the transformation task when $\Psi_{rd}^{fr} \neq 0$ which only occurs when the system is at zero energy. At this point, any value can be assigned to the flux in equations (4.4) and (4.5), because this situation exists only for a very short time, during startup.

The flux orientation is handled through the Park transformation [7], to which the needed flux angle is computed from the real and imaginary part of the estimated flux vector. It is clear that for accurate operation we need a very good estimation of the real flux. This is the main reason, why such a complex structure is used for the estimation task. Even in noisy environment, the H_∞ observers are capable for this very accurate estimation because of their low-pass property. Thus for the stator oriented LPV flux model of the IM:

$$\frac{d}{dt}\begin{bmatrix}\Psi_{r\alpha}^s \\ \Psi_{r\beta}^s\end{bmatrix} = \begin{bmatrix}-p_2/L_r & -p_1 \\ p_1 & -p_2/L_r\end{bmatrix} \cdot \begin{bmatrix}\Psi_{r\alpha}^s \\ \Psi_{r\beta}^s\end{bmatrix} + \begin{bmatrix}L_m p_2/L_r & 0 \\ 0 & L_m p_2/L_r\end{bmatrix} \cdot \begin{bmatrix}i_{r\alpha}^s \\ i_{r\beta}^s\end{bmatrix}, \tag{4.6}$$

the MS structure on *Figure 8* was used to calculate an H_∞ observer with the *hinfgs* function. In this structure we chose the frequency of the nonfiltered deviations to be greater than 300Hz, so the introduced sensitivity filter was

$$\mathbf{W}_S(s) = \mathrm{diag}\left(300/\left(s+30\right), 300/\left(s+30\right)\right). \tag{4.7}$$

Because any kind of disturbance can shock the system $\mathbf{W}_w(s)$ was omitted for wide interval of functioning. The resulted observer had a $\gamma = 8.49 \cdot 10^{-5}$. Although, this observer calculates the flux vector we still need ω and R_r. To obtain their value, an EKF is attached to the observer. This EKF based on (2.1), (2.3), (2.5) nonlinear equations, where $u_{s\alpha}^s$, $u_{s\beta}^s$, T_{load} is used as known inputs and $i_{s\alpha}^s$, $i_{s\beta}^s$ as the measured outputs of the system. Because of the strong dynamical properties of the resulted model, the prediction phase (see [2]) of this EKF is computed trough a 3rd order recursive Adams-Bashforth numerical method [10], and in its correction phase only the diagonal elements of **Q** (expected variance of the system noise) and **R** (expected variance of the measurement noise) were chosen to be nonzeros. It is not a strict assumption, because there is no significant cross coupling between these noises in the real environment. For this reason

$$\mathbf{Q}_{ij} = 0, \text{ expect } \mathbf{Q}(i_{s\alpha}^s, i_{s\alpha}^s) = \mathbf{Q}(i_{s\beta}^s, i_{s\beta}^s) = 0.0117h/\left(L_s\sigma\right); \quad i,j \in \{0,1,..,6\} \tag{4.8}$$

$$\mathbf{R}_{ij} = 0, \text{ expect } \mathbf{R}(\Psi_{r\alpha}^s, \Psi_{r\alpha}^s) = \mathbf{R}(\Psi_{r\beta}^s, \Psi_{r\beta}^s) = 0.0205,$$
$$\mathbf{R}(i_{s\alpha}^s, i_{s\alpha}^s) = \mathbf{R}(i_{s\beta}^s, i_{s\beta}^s) = 13.85; \quad i,j \in \{0,1,\ldots,4\} \tag{4.9}$$

where h is the step size of the numerical algorithm. The whole estimation structure was tuned to be perfectly functioning with only 0.5% of prediction error, while heavy measurement noise (*Figure 9*), inverter noise (*figure 10*) and 5% parameter uncertainties was introduced into the Matlab simulations, during the design.

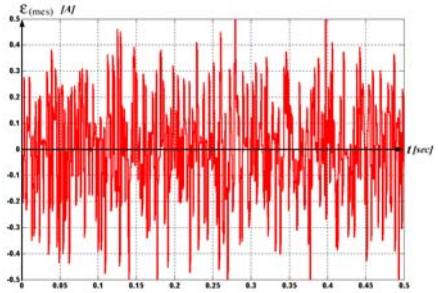

Fig. 9. Modeled measurement noise during design

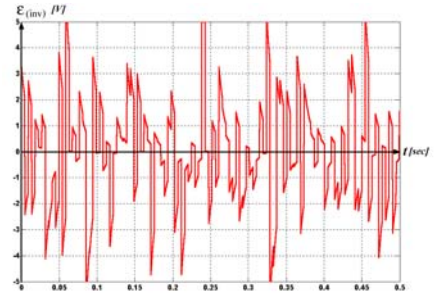

Fig. 10. Modeled inverter noise during design

V. Simulation And Test Results

The controller was tested in Matlab with the help of an IM Simulink model. During a very dynamic

task where the load torque changed as in *Figure 13*, the reference tracking for speed occurred as in *Figure 11* when the rotor flux was changing as in *Figure 12*.

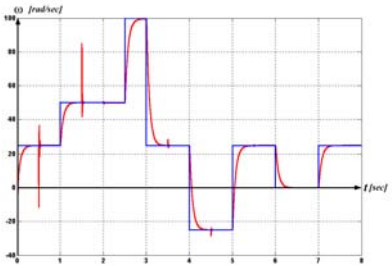

Fig. 11. Reference tracking for ω

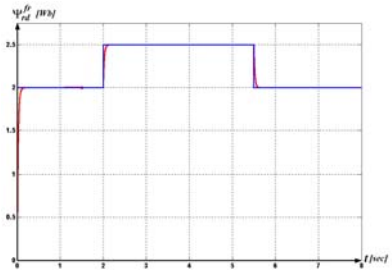

Fig. 12. Reference tracking for Ψ_{rd}^{fr}

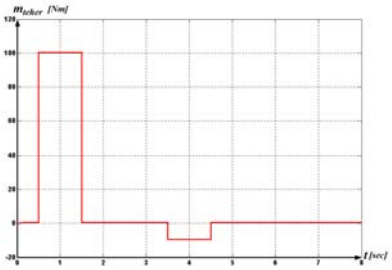

Fig. 13. Change of T_{load}

Figure 14 and *Figure 15*.shows the stator voltages, during the simulation

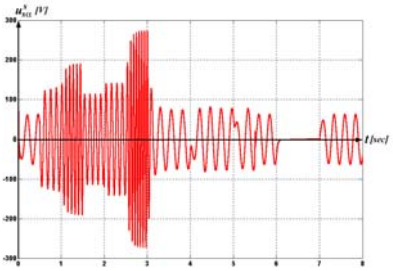

Fig. 14. Change of $u_{s\alpha}^{s}$

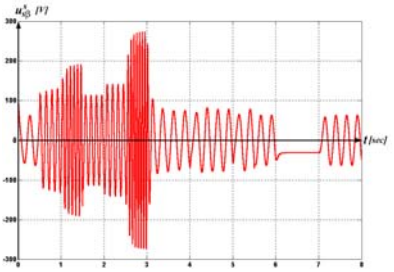

Fig. 15. Change of $u_{s\beta}^{s}$

Looking to these results can be concluded that the controller works well even in rapidly changing load conditions (like at 0.5 msec) and its tracking accuracy and dynamics even for large reference steps (like at 3.5 mesc) are good. The controller was also tested for robustness. With 5% of parameter variance the maximum tracking error in speed was no more than 10%.

IV. Implementation With TMS320F243

The proposed controller is under implementation on a Digital Spectrum motion control development kit which is powered by a TMS320F243 DSP. This fixed point DSP processor is capable of 20Mips and the processors board contains 8K word Flash ROM. This hardware directly connects to an inverter interface card which produces the PWM signals for a $300V_{pp}$ AC capable inverter that empowers the IM seen on *Table 1*. This interface card also contains analog to digital converters (ADC) which are used to get to know the values of the stator currents and of course is responsible to directly give the PWM signals to the inverter. The connection of the structure is presented on *Figure 11*.

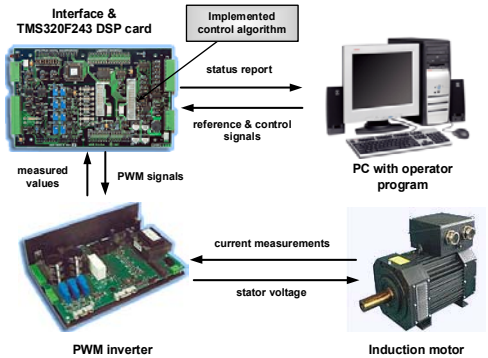

Fig. 16. Implemented AC drive with DSP control

The program of the DSP card is developed in Code Composer. During implementation the continues controller system was discretised with

the Euler method with a chosen step size of 1msec, considered enough to represent the continuous controller. Even with the drawback of the fixed point calculations the implementation shows acceptable performance. (The measurements of the performance will be given in the final paper)

VII. Conclusion

In this paper our aim was to show the design steps of a state of the art controller for speed sensorless robust operation of the IM, taking into account the load torque changes without the loss of reference accuracy and (effectiveness)??? of the whole drive. It is clearly turned out, that with the use of the MS LPV H_∞ control theory the proposed task can be handled and even implemented on a cheap hardware. However, this structure gives the opportunity of control of a given IM with a parameter variance no more than 5%, its usage would be greatly improved with an online tuning algorithm which is in the focus of our future research.

Notations

(**A**, **B**, **C**, **D**, **E**) Matrices of the state space representaion of a system

IM Induction Motor MS Mixed Sensitivity

EKF Extended Kalman Filter DSP Digital Signal Processor

LPV Linear Parameter Variant RFO Rotor Field Orientation

LTILinear Time Invariant PWM Pulse Width Modulation

References

[1] Åström K. J., and B. Wittenmark: Computer Controlled Systems, *Prentice-Hall*, 1990.

[2] Hartung F.: Introduction to Numerical Analyses, *in hungarian, Veszprémi Egyetem*, 1998.

[3] Hilairet M., C. Darengosse, F. Auger, and P. Chevrel: Sysnthesis and Analysis of Robust Flux Observers for Induction Machines, *Bd. de l'Université*, France (2000).

[4] Holtz J.: The Representation of AC Machine Dynamics by Complex Signal Flow Graphs, *IEEE Transactions on Industrial Electronics*, Vol. 42, No. 3, (1995), pp. 263-271.

[5] Holtz J.: Sensorless Control of Induction Drives, *Proceedings of the IEEE*, Vol. 90, No. 8, (2002), pp. 1259-1394.

[6] Kálmán R. E.: A New Approach to Linear Filtering and Prediction Problem, *Journal Basic Engineering*, Vol. 82, (196), pp. 34-45.

[7] Kovács P.K.: Transient Phenomena in Electrical Machines, *Akadémiai kiadó*, 1954.

[8] Fodor D., L. Szalay, and K. Bíró: H_∞ Output Feedback Controller Design for AC Motor Control, *Proceedings of 10th International Power Electronics and Motion Conference*, EPE-PEMC 2002, Dubrovnik & Cavat.

[9] Lee C. H., M. H. Shin, and M. J. Chung: A Design of Gain-Scheduled Control for a Linear Parameter Varying System: An Application to Flight Control, *Control Engineering Practice*, No. 9, (2001), pp. 11-21.

[10] Premapain E., I. Pstletwaite, and A. Benchaib: A Linear Parameter Variant H_∞ Control Design for an Induction Motor, *Control Engineering Practice*, No. 10, (2002), pp. 663-644.

[11] Skogestad S., and I. Postletwaite: Multivariable Feedback Control, *John Wiley & Sons*, 1996.

[12] Uray V.: Elektrotechnics, in hungarian, *Műszaki könyvkiadó*, 1970.

[13] Vas P.: Sensorless Vector and Direct Torque Control, *Oxford University Press*, 1998.

[14] Zames G.: Feedback and Optimal Sensitivity: Model Reference Transformations, Multiplicative Seminorms and Approximate Inverse, *IEEE Transactions on Automatic Control*, Vol. 26, No. 1, (1981), pp. 301-320.

[15] Zhou K., and J. C. Doyle: Essentials of Robust Control, *Prentice-Hall*, 1998.

Description	Nominal value
Lumped stator 3 phase inductance	0.13 H
Lumped rotor 3 phase inductance	0.13 H
Lumped mutual 3 phase inductance	0.12 H
Leakage factor	0.15
Stator 3p. resistance	1.86 Ω
Rotor 3p. resistance	[3Ω, 6Ω]
R_r at T_0 temperature	3Ω
Shaft rotor speed	[-85Hz, 100Hz]
Rotor flux frequency	[-50Hz, 50Hz]
Load torque	[-100Nm, 100Nm]
Rotor winding weight	4 kg
Specific heat ct. (Al)	0.21
Nominal temperature	18º
Moment of inertia	0.21 J/kgK
Number of pole pairs	3
Fraction	0.001
Linear heat convection	3.5

$i_{sx}(t)$	Stator x phase current [A]	$\mathbf{x}^{s}$	Stator oriented space phasor
$u_{sx}(t)$	Stator x phase voltage [V]	$\mathbf{x}^{fr}$	Rotor field oriented space phasor
Ψ	Magnetic flux [Wb]	x_{d}	Re part of $\mathbf{x}^{fr}$ space phasor(rotating)
$\mathbf{i}_{s}^{x}(t)$	Stator current space phasor [A]	x_{q}	Im part of $\mathbf{x}^{fr}$ space phasor
$\mathbf{i}_{r}^{x}(t)$	Rotor current space phasor [A]	x_{α}	Re part of $\mathbf{x}^{s}$ space phasor (stacionary)
$\mathbf{\Psi}_{s}^{x}(t)$	Stator flux space phasor [Wb]	x_{β}	Im part of $\mathbf{x}^{s}$ space phasor
$\mathbf{\Psi}_{r}^{x}(t)$	Rotor flux space phasor [Wb]	x_{ref}	Reference signal for x
$\mathbf{u}_{s}^{x}(t)$	Stator voltage space phasor [V]	$x_{(error)}$	Tracking error for x
$\mathbf{i}_{s}^{x}(t)$	Stator current space phasor [A]	h	Discrete time step [sec]
$\mathbf{u}_{r}^{x}(t)$	Rotor voltage space phasor [V]	$\boldsymbol{\varepsilon}_{inv}(t)$	Inverter noise [V]
$i_{eff}^{r}(t)$	Effective value of $i^{r}(t)$ [A]	$\boldsymbol{\varepsilon}_{mes}(t)$	Measurement noise [A]
P	General problem (state space modell)	t	Time [sec]
$\breve{\mathbf{P}}$	Mixed-sensitivity system	**K**	Controller (state space modell)
G(**s**)	Transfer function of the system	γ	Optimal H_{∞} norm
x	State vector of **P**	v_1, v_2	Virtual inputs
y	Output vector of **P**	**p**	Parameter vector
u	Input vector of **P** (controlable)	$\mathbf{W}_{x}$	Filter for transfer function x
v	Output vector of **P** (measured)	**S**	Sensitivity transfer function
z	Output vector of **P** (optimalized)	**T**	Inverz-sensitivity transfer function
w	Disturbances of **P**	**KS**	Transfer function of the closed loop
r	Reference signals of **P**	**R**	Variance of $\boldsymbol{\varepsilon}_{mes}(t)$
n / **d**	Noises of **P**	**Q**	Variance of $\boldsymbol{\varepsilon}_{inv}(t)$